Published online 16 December 2014 *Nucleic Acids Research, 2015, Vol. 43, No. 1* **607–617**
doi: 10.1093/nar/gku1325

NERF encodes a RING E3 ligase important for drought resistance and enhances the expression of its antisense gene *NFYA5* in *Arabidopsis*

Wei Gao†, Wenwen Liu†, Meng Zhao and Wen-Xue Li*

National Key Facility for Crop Gene Resources and Genetic Improvement, Institute of Crop Science, Chinese Academy of Agricultural Sciences, Beijing 100081, China

Received June 05, 2014; Revised November 25, 2014; Accepted December 07, 2014

ABSTRACT

***NFYA5* is an important drought-stress inducible transcription factor gene that is targeted by miR169 in *Arabidopsis*. We show here that the *cis*-natural antisense transcript gene of *NFYA5*, *NFYA5 Enhancing RING FINGER* (*NERF*), can produce siRNAs from their overlapping region (OR) and affect *NFYA5* transcripts by functioning together with miR169. The NERF protein functions as an E3 ligase for ubiquitination. Overexpression of *NERF* or *OR* cDNA leads to siRNANERF accumulation, miR169 repression, and *NFYA5* transcript enhancement; knockdown of *NERF* transcripts by an artificial miRNA enhances miR169 abundance and reduces *NFYA5* transcripts. Overexpression of *NFYA5* does not affect the *NERF* mRNA level. Deep sequencing of the small RNA library from *35S::OR* plants identifies 960 sequences representing 323 unique siRNAs that originate from *OR*; the sequences of some siRNANERF are similar/complementary to those of miR169. Overexpression of the 195- to 280-bp *OR* cDNA-containing siRNAs similar/complementary to miR169 also leads to the accumulation of *NFYA5* transcripts. Analysis of *NERF* knock-down plants and *NERF* overexpression lines showed that, like *NFYA5*, *NERF* is important for controlling stomatal aperture and drought resistance. This regulatory model might apply to other natural antisense transcripts with positively correlated expression patterns.**

INTRODUCTION

Small RNAs regulate gene expression through post-transcriptional gene silencing, translational inhibition or heterochromatin modification (1). Small RNAs can be classified into 20- to 24-nucleotide (nt) microRNAs and endogenous short interfering RNAs (siRNAs), such as 21-nt ta-siRNAs (*trans*-acting siRNAs), ∼24-nt repeat-associated siRNAs, and 21- or 24-nt nat-siRNAs. miRNAs are processed from hairpin precursors by the ribonuclease III-like enzyme Dicer-like in plants. siRNAs differ from miRNAs in that they are generated from long, double-stranded RNAs, including transcribed repeat sequences, products of RNA-dependent RNA polymerase, and natural antisense transcripts (NATs) (2,3).

NATs are RNA molecules that are transcribed from the opposite DNA strand compared with other transcripts and overlap in part with sense RNA (4). There are two kinds of NATs: *cis*-NATs and *trans*-NATs. *cis*-NATs are formed by antisense transcripts at the same genomic locus, whereas the sense and antisense transcripts of *trans*-NATs are derived from different genomic loci (5). *cis*-NATs have been detected in most species analyzed, and the reported frequencies for overlapping gene pairs in different species range from 5 to 10%. In the human genome, 4 to 9% of all transcripts overlap, while >20% genes have been reported to be overlapping in *Drosophilia*. In plants, *cis*-NATs have been analyzed in rice and *Arabidopsis* (1,5,6). In *Arabidopsis*, 1340 potential *cis*-NAT pairs have been predicted, and 957 *cis*-NATs have been confirmed to be sense and antisense transcripts by analysis of full-length cDNAs and massively parallel signature sequencing data (7).

cis-NATs mediate inhibition of microRNA function in humans (8). In plants, *cis*-NATs are thought to be important for the biogenesis of nat-siRNAs, and genome-wide analysis has demonstrated the widespread existence of nat-siRNAs in plants (9–11). nat-siRNAs could be the main modulators of gene regulation in plants as suggested by research on the NaCl-inducible nat-siRNASRO5 (12), pathogen-related nat-siRNAATGB2 (13), and sperm-specific nat-siRNAKPL (14). These nat-siRNAs usually cause silencing of the antisense transcript and lead to the anti-correlated expression pattern of NATs (7,9,11). However, independent researchers have reported that *cis*-NATs do not tend to produce nat-siRNAs when compared to non-

*To whom correspondence should be addressed. Tel: +86 10 82105799; Email: liwenxue@caas.cn
†These authors contributed equally to the paper as first authors.

overlapping neighboring gene pairs, and anti-correlated expression of *cis*-NATs represent only a small number of the total *cis*-NATs (5,15,16). Thus, the mechanisms by which NATs regulate gene expression remain poorly understood.

Regulation of gene expression at the transcriptional level is crucial for normal development and physiology in plants (17,18). We previously reported that the transcription factor *NFYA5* is important for drought resistance in *Arabidopsis*, and that drought stress up-regulates *NFYA5* gene expression not only at the transcriptional level but also at the post-transcriptional level by down-regulating the expression of miR169a that targets *NFYA5* transcript for cleavage (19). *NFYA5* is annotated to overlap with *NERF* (NFYA5 Enhancing RING FINGER) on the antisense strand in their 3′ UTR regions to form a *cis*-NAT gene pair. In several cases, a change in the expression of the E3 ubiquitin ligase gene altered drought resistance and plant hormone action by regulation of down-stream target genes. For example, overexpression of *SDIR1* (salt- and drought-induced RING finger 1) led to ABA hypersensitivity and ABA-associated phenotypes, such as salt hypersensitivity in germination, enhanced ABA-induced stomatal closing, and enhanced drought tolerance (20); and *35S::Rma1H1* (RING membrane-anchor 1 homolog 1) transgenic *Arabidopsis* became more resistant to drought stress via the down-regulation of plasma membrane aquaporin levels by inhibiting aquaporin trafficking to the plasma membrane and subsequent proteasomal degradation (21).

Here, we show that *NERF* functions as a RING finger protein that has ubiquitin E3 ligase activity. Transcriptional levels of *NERF* positively affect *NFYA5* mRNA abundance by antagonizing miR169 expression through siRNANERF originating from the *NERF* and *NFYA5* overlapping region (*OR*). Expression of *NERF* in vascular tissues and guard cells, and analysis of *NERF* knock-down plants and *NERF* overexpression lines show that, like *NFYA5*, *NERF* is pivotal in controlling stomatal aperture and drought resistance.

MATERIALS AND METHODS

Plant materials and growth conditions

Arabidopsis thaliana ecotype Columbia (Col-0) was used as the wild type (WT) and was the genetic background for transgenic plants. *dcl2/3/4* and other mutants involved in the small RNA biogenesis pathway were maintained in our laboratory. These mutants were in the Col-0, *Landsberg erecta* (Ler), Nosssen-0 (No), or C24 genetic backgrounds as indicated in the text and figures. *Arabidopsis* plants were grown under 16 h light/8 h dark at 23 ± 1°C. For drought treatment, plants were grown in soil with sufficient water for 3 weeks, and then the water was withheld for the indicated durations.

Constructs and generation of transgenic plants

The cDNAs of *NERF* with/without 3′ UTR, *NFYA5* with 3′ UTR, and *OR* and *ORC* fragments were amplified by PCR. The corresponding products were introduced into the pENTR™/D-TOPO vector (Invitrogen) and cloned into pMDC32 by LR reactions (Invitrogen). The schematic diagrams of *OR* and *ORC* amplicons are provided in Supplementary Figure S1.

To generate *NERF* knockdown *Arabidopsis* plants, we engineered a gene-specific amiRNA by replacing the original miR319a sequence in the pRS300 plasmid as previously described (22). The constructs were cloned into the pCPB vector behind the cauliflower mosaic virus (CaMV) *35S* promoter using the BamHI restriction site by In-Fusion reaction.

For the *NERF* promoter::GUS construct, a 1.4-kb fragment of the full inter-region between the stop codon of At1g54130 and the initiation codon of *NERF* was amplified and cloned into the pMDC164 vector following Gateway recombination.

A fusion of yellow fluorescence protein (YFP) to the C-terminal end of NERF was generated and introduced into the pEarleyGate101 vector by Gateway recombination. YFP images were collected on a Leica SP2 confocal microscope.

The plasmid was electroporated into *Agrobacterium tumefaciens* GV3101 and was transformed into *Arabidopsis* by the floral dip method (23). Transgenic plants were selected with the use of 35 μg ml^{-1} hygromycin or 45 μM PESTANAL. T3 or T4 homozygous lines were used for all experiments. The sequences of the primer pairs used in the experiments are listed in Supplementary Table S1.

RNA analysis

Total RNA was extracted from WT and transgenic plants with Trizol reagent (Invitrogen). For enrichment of small RNAs, high molecular weight RNA was selectively precipitated by the addition of one volume of 20% PEG 8000/1M NaCl and separated on 1.2% formaldehyde-MOPS agarose gels for northern blot. The probes were labeled with ^{32}P-dCTP using a Ready-To-Go DNA Labeling Kit (Amersham Biosciences). Low molecular weight RNA was fractionated on 17% denaturing polyacrylamide gels, and small RNA northern blots were probed and washed as described (19) except for *OR* cDNA, which was labeled using similar methods to northern blot.

For real-time RT-PCR, 5 μg of total RNA isolated with the RNeasy plant mini kit was used for the first-strand cDNA synthesis using SuperScript III first-strand synthesis supermix (Invitrogen). The cDNA reaction mixture was diluted 50 times, and 3 μl was used as template in a 25-μl PCR reaction. PCR included a pre-incubation at 95°C for 3 min, followed by 40 cycles of denaturation at 95°C for 15 s, annealing at 58°C for 40 s, and extension at 72°C for 40 s. All the reactions were carried out in an ABI 7500 system (Applied Biosystems) using the SYBR Premix Ex Taq™ (perfect real time) kit (TaKaRa Biomedicals). Primer efficiencies were measured and calculated (24). The PCR products were loaded on 1.5% agarose gels and photographed after staining with ethidium bromide. Each experiment was replicated three times. The comparative Ct method was applied.

Small RNA library construction, sequencing and data analysis

The miRNAs were cloned as described by Sunkar and Zhu with some modifications (25). In brief, low molecular weight RNA was fractionated on 17% denaturing polyacrylamide gels. Small RNAs in the range of 16-30 nt were excised and eluted with 0.3 M NaCl. The RNA was dephosphorylated and ligated sequentially to 5′ and 3′ RNA/DNA chimeric oligonucleotide adaptors. Reverse transcription PCR was carried out, and the resulting PCR products were sequenced using Solexa sequencing technology (BGI, Shenzhen, China).

The raw reads were produced after excluding low quantity reads and 5′ and 3′ adaptor contaminants. The identical adaptor-trimmed sequences in the range of 1630 nt were grouped as unique sequences with normalized counts for the individual sequence reads. The unique small RNAs were aligned to the *NERF* and *NFYA5* overlapping region.

5′ RACE

To obtain cleavage fragments resulting from transcript processing by microRNAs, we used the 5′ RACE System for Rapid Amplification of cDNA Ends, Version 2.0 (Invitrogen). Total RNA was extracted from 10-day-old *35S::OR* seedlings using the TRIZOL method described above. The oligo(dT) was then used for cDNA synthesis. Initial PCR was carried out using the 5′ RACE Abridged Primer and gene specific outer primer (5′-GTA ATG CAA TTG TAC TCT CGA G-3′). Nested PCR was carried out using 1/100 of the initial PCR reaction as template, Universal Amplification Primer, and gene-specific inner primer (5′-AGA GAA TCG GAA GTT AAC AAA ATA G-3′). RACE fragments were cloned and sequenced after gel purification.

Ubiquitination assays

The coding region of *NERF* was cloned into the pGEX-4T-3 vector by BamHI and NotI sites and expressed in *Escherichia coli*. The recombinant fusion protein was purified with a B-PER® GST Spin Purification Kit (Thermo Scienfic). Site-directed mutagenesis was performed to generate NERF with a mutated RING function domain with a QuickChange II Site-Directed Mutagenesis Kit (Stratagene). This fragment was sequenced to ensure that only the desired mutations were introduced. The sequences of the primer pair used for the preparation of the WT, H348Y and C367S mutants are listed in Supplementary Table S1.

The ubiquitination assays were performed in the presence of E1, E2 and flag-ubiquitin as described by Xie *et al.* (26). Approximately 500 ng of GST-NERF fusion protein was used in the mixture of 40 ng of rabbit E1 (Boston Biochemicals), 40 ng of human UbcH5b (Boston Biochemicals), and 1 μg of flag-ubiquitin (Boston Biochemicals). The reaction mixture was incubated in 50 mM Tris-HCl (pH 7.4), 2 mM ATP, 5 mM $MgCl_2$, and 2 mM DTT for 2 h at 30°C with agitation in an Eppendorf Thermomixer. Samples were then heated to 95°C in a buffer containing 2-mercaptoethanol before separation by SDS-PAGE and immunoblot analysis using anti-flag antibody.

Stomatal aperture analysis

For the determination of stomatal aperture responses to drought stress, rosette leaves were obtained from 3-week-old soil-grown plants at similar developmental stages that had been provided with/without sufficient water. The leaves were harvested in the morning 2 h after they were exposed to light. Leaves were immediately frozen in liquid nitrogen, and their guard cells were observed by environmental scanning electron microscopy (HITACHI, TM 1000). The width and length of stomatal pores were measured.

RESULTS

NERF protein functions as an E3 ligase for ubiquitination

Previously, Borsani *et al.* reported a new type of endogenous siRNA derived from a NAT pair and described its role in salt tolerance in *Arabidopsis* (12). This motivated us to investigate *NERF* (At1g54150) because it formed a *cis*-NAT with *NFYA5* in their 3′ UTR regions (Supplementary Figure S1), and because we have demonstrated the critical functions of *NFYA5* in drought resistance in *Arabidopsis* (19). The C terminus of NERF contains a C3-H-C4 RING finger domain comprising conserved Cys and His residues (Figure 1A). To determine whether this RING finger protein has E3 ligase activity, we performed an *in vitro* self-ubiquitination assay. We expressed *NERF* in *E. coli* as a fusion protein with glutathione-*S*-transferase (GST) and subsequently obtained affinity purified GST-NERF (Figure 1B). In the presence of rabbit E1 and a human E2, polyubiquitinated proteins were formed (Figure 1C), verifying that this ubiquitination activity depends on the presence of GST-NERF as well as E1 and E2. To determine whether the RING domain is required for NERF E3 ligase activity, we constructed two single amino acid alleles by mutagenizing the conserved amino acid His-348 to Tyr (H348Y) and Cys-367 to Ser (C367S), which presumably disrupted the RING finger domain (Figure 1A). *In vitro* self-ubiquitination assay showed that neither mutant protein had significant ubiquitin ligase activity (Figure 1D), demonstrating that the RING domain is required for NERF E3 ligase activity.

Expression patterns of *NERF*

Semi-quantitative RT-PCR indicated that *NERF* was expressed in various tissues, including roots, stems, flowers and leaves (Figure 2A). We also constructed promoter::GUS transgenic lines to examine the expression patterns of *NERF*. Analysis of GUS staining patterns in several transgenic lines showed that the promoter was active in cotyledons, root vascular tissue and root tips of 8-day-old seedlings (Figure 2B, panels I and II). GUS staining was also observed in flowers and siliques (Figure 2B, panels III and IV), confirming that the *NERF* promoter, like *NFYA5*, was active at all developmental stages. Importantly, the *NERF* expression was detected in guard cells (Figure 2B, panels V), which is also consistent with the location of *NFYA5* (19).

The Psort program predicted a membrane localization of NERF protein, with 83% certainty for its location in the mitochondrial inner membrane or 60% certainty for its location in the plasma membrane (http://psort.ims.u-tokyo.

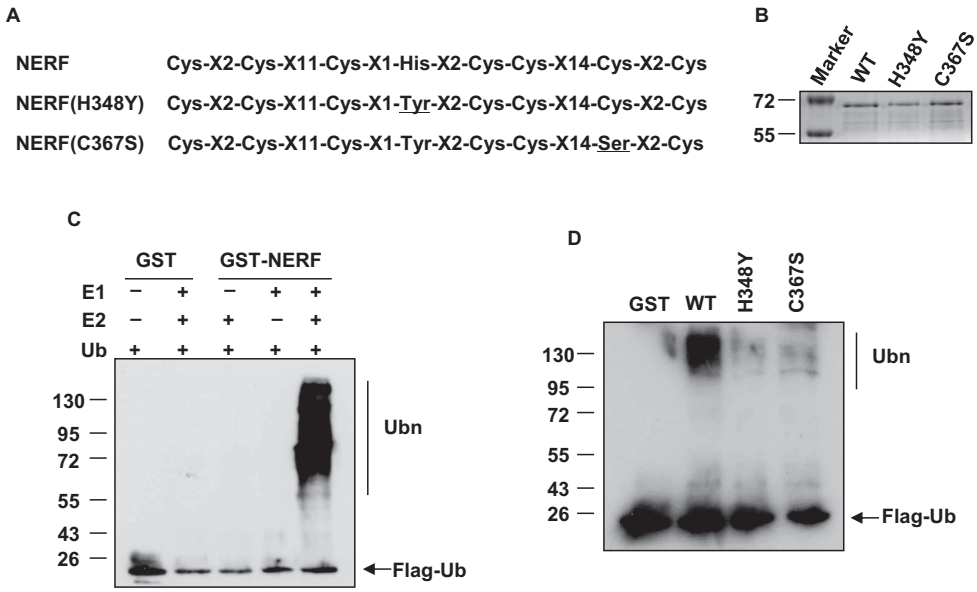

Figure 1. E3 ubiquitin ligase activity of NERF and the RING mutant variants. (**A**) Amino acid sequences of the NERF Ring finger and the RING mutant variants. The mutated residues in NERF are underlined. (**B**) Purified recombinant proteins were fractioned by SDS-PAGE. The numbers at the left indicate the molecular masses of marker proteins in kilodaltons. (**C**) GST-NERF was assayed for E3 activity in the presence of E1 (from rabbit), E2 (UBCh5b), and flag-tag ubiquitin (Ub), as indicated. The numbers at the left indicate the molecular masses of marker proteins in kilodaltons. Samples were resolved by 10% SDS-Page and were detected by anti-flag immune blot analysis. The free ubiquitin and polyubiquitinated GST-NERF are indicated. (**D**) GST-NERF E3 activity depended on its RING motif. Wild-type GST-NERF and mutants (H348Y and C367S) were assayed for self-ubiquitination in the presence of E2 (UBCh5b), E1 and flag-tag ubiquitin.

ac.jp/form.html). To confirm the subcellular localization of NERF protein, we transformed *Arabidopsis* with a translational fusion between YFP and the C terminus of NERF under the control of the CaMV *35S* promoter. In contrast to the prediction by the Psort program, root cells expressing the NERF fusion protein showed that the YFP signal mainly appeared in the nucleus as *NFYA5* and was only weakly evident outside the nuclear compartment (Figure 2C).

To determine whether *NERF* expression was also regulated by water stress, as is the case with *NFYA5* (19), we subjected 20-day-old *Arabidopsis* seedlings to dehydration treatments and then isolated the corresponding RNA for RNA gel blot analysis. The transcripts of *NERF* were induced by the dehydration treatment. The relative level of *NERF* expression was about 3-times greater after 6 h of dehydration treatment than in the control, suggesting that *NERF* is involved in stress responses (Figure 2D).

Transcriptional levels of *NERF* positively affect *NFYA5* mRNA abundance

The similar expression patterns for *NERF* and *NFYA5* prompted us to investigate whether the expression of the two genes is correlated. We first searched the publicly available T-DNA collections and obtained a T-DNA insertion line in *NERF* from the Arabidopsis Biological Resource Center, SALK_096716. Plants homozygous for the T-DNA insertion were identified by PCR, and sequencing of the T-DNA flanking region confirmed the insertion site in the promoter region of *NERF* (Supplementary Figure S2). However, the *NERF* transcripts in WT and SALK_096716 were similar (Supplementary Figure S2). Thus, an artificial miRNA targeting *NERF* mRNA was designed following the strict base-pairing rules described by Schwab (22) and using the designing tool at http://wmd3.weigelworld.org/cgi-bin/webapp.cgi. Artificial miRNA was then introduced into *Arabidopsis* (Figure 3A), and its effectiveness in silencing *NERF* expression was verified by real-time RT-PCR. Two independent *amiNERF* lines were chosen for further analysis (Figure 3A). Like *NERF* transcripts, the *NFYA5* transcripts were significantly decreased in *amiNERF* transgenic plants, i.e., the level of *NFYA5* mRNA was ∼40% lower in *amiNERF* plants than in the WT (Figure 3A).

To further characterize the possible relationship between *NERF* and *NFYA5*, we generated transgenic *Arabidopsis* plants overexpressing the full-length cDNA of *NERF* and tested the *NFYA5* transcripts in the corresponding transgenic lines (Figure 3B). Contrary to the down-regulation of *NFYA5* transcripts in *amiNERF* plants, the mRNA abundance of *NFYA5* significantly increased in *35S::NERF* transgenic plants, and the *NFYA5* level was positively correlated with the expression of *NERF* (Figure 3B). *NFYA5* transcripts did not accumulate in *35S::NERF-cds* (without 3′-UTR) transgenic plants, suggesting that 3′-UTR or the *OR* is essential for the accumulation of *NFYA5* in *35S::NERF* transgenic plants (data not shown). To test this hypothesis, we constructed transgenic plants only overexpressing *OR* cDNA, and quantified the effects of *OR* overexpression on *NFYA5* transcripts (Figure 3B). The *NFYA5* transcripts were significantly enhanced in *35S::OR* transgenic plants (Figure 3B), demonstrating that *OR* is essential for the accumulation of *NFYA5* transcripts in *35S::NERF* transgenic plants.

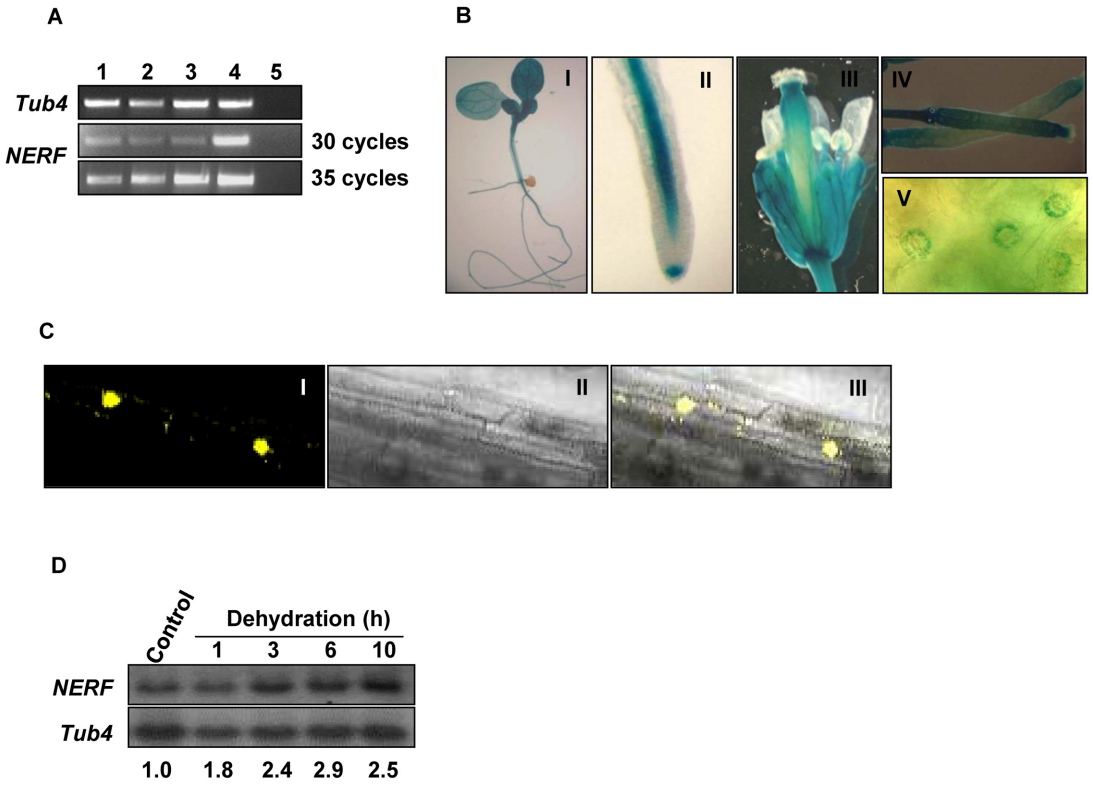

Figure 2. *NERF* expression patterns. (**A**) Semi-quantitative RT-PCR analysis revealed the constitutive expression of *NERF* in various tissues, including root (lane 1), flower (lane 2), stem (lane 3) and leaf (lane 4). The *Tub4* gene was used as a positive control. No bands were detected in the minus RT controls (lane 5). (**B**) *NERFp*::GUS expression patterns in various tissues. The staining was prominent in leaf and root vascular tissues (I), root tips (II), inflorescence (III), siliques (IV) and guard cells (V). (**C**) Subcellular localization of NERF. NERF-YFP fusion construct was expressed in transgenic *Arabidopsis* under the control of the CaMV *35S* promoter, and the plant roots were observed with a confocal microscope. The roots were photographed in the dark field for yellow fluorescence (I), in the bright field for the morphology of the cells (II), and in combination (III). (**D**) Regulation of *NERF* mRNA abundance by dehydration shock. A 20-μg quantity of total RNA from each sample was loaded and hybridized with ^{32}P-labeled full-length *NERF* probe. *Tub4* was used as a loading control. Numbers below each lane indicate the expression level of *NERF* relative to *Tub4*.

In *Arabidopsis* and *Medicago truncatula*, the expression of *NFYA5* is mainly regulated by miR169 at the post-transcriptional level (19,27). To determine whether the down-/up-regulation of *NFYA5* in *amiNERF*, *35S::NERF* and *35S::OR* transgenic plants is due to the variation in miR169 expression, we isolated small RNA from *amiNERF, 35S::NERF* and *35S::OR* transgenic plants. Compared to its expression in WT, the expression of miR169 was significantly up-regulated in *amiNERF* plants, and significantly down-regulated in *35S::NERF* and *35S::OR* transgenic plants (Figure 3C), indicating that the changes in the levels of *NFYA5* transcripts in *amiNERF*, *35S::NERF* and *35S::OR* transgenic plants were at least partly due to the variation of miR169 abundance.

Overexpression of *NFYA5* does not increase *NERF* expression

Significant variations of *NFYA5* mRNA abundance in *amiNERF*, *35S::NERF* and *35S::OR* transgenic plants prompted us to test whether *NFYA5* transcripts could affect the expression of *NERF*. We generated transgenic *Arabidopsis* plants overexpressing *NFYA5* with 3′ UTR (Figure 4A). Overexpression of *NFYA5* did not affect the expression of *NERF* (Figure 4A). Correspondingly, we did not observe obvious variation in miR169 accumulation between WT and *35S::NFYA5* transgenic plants (Figure 4B), suggesting that it is the special strand in *OR* between *NERF* and *NFYA5* that affects the expression level of miR169.

siRNANERF biogenesis

When the *OR* cDNA was used as a probe and the hybridization temperature was increased to 45°C to improve the specificity of the signal, a small RNA signal around 21 nt was detected in WT and transgenic plants and significantly accumulated in *35S::NERF* transgenic plants (Figure 5A). Because the stem-loop structure, which is the basic criterion for identification of plant microRNAs (28), did not exist in *OR* predicted by Mfold (29), we deduced that the small RNAs originated from *OR* were siRNAs, and we designated them siRNANERF. The siRNANERF level was also significantly enhanced in *35S::MIR169a* transgenic plants compared to the WT (Supplementary Figure S3), indicating that siRNANERF and miR169 might have similar sequences.

To confirm that siRNANERF can regulate *NFYA5* expression, we carried out modified 5′ RACE using mRNA from *35S::OR* transgenic plants in order to map the potential cleavage sites of *NFYA5* (Figure 5B). Although it was detected at only a low frequency (4 of 20), one site between

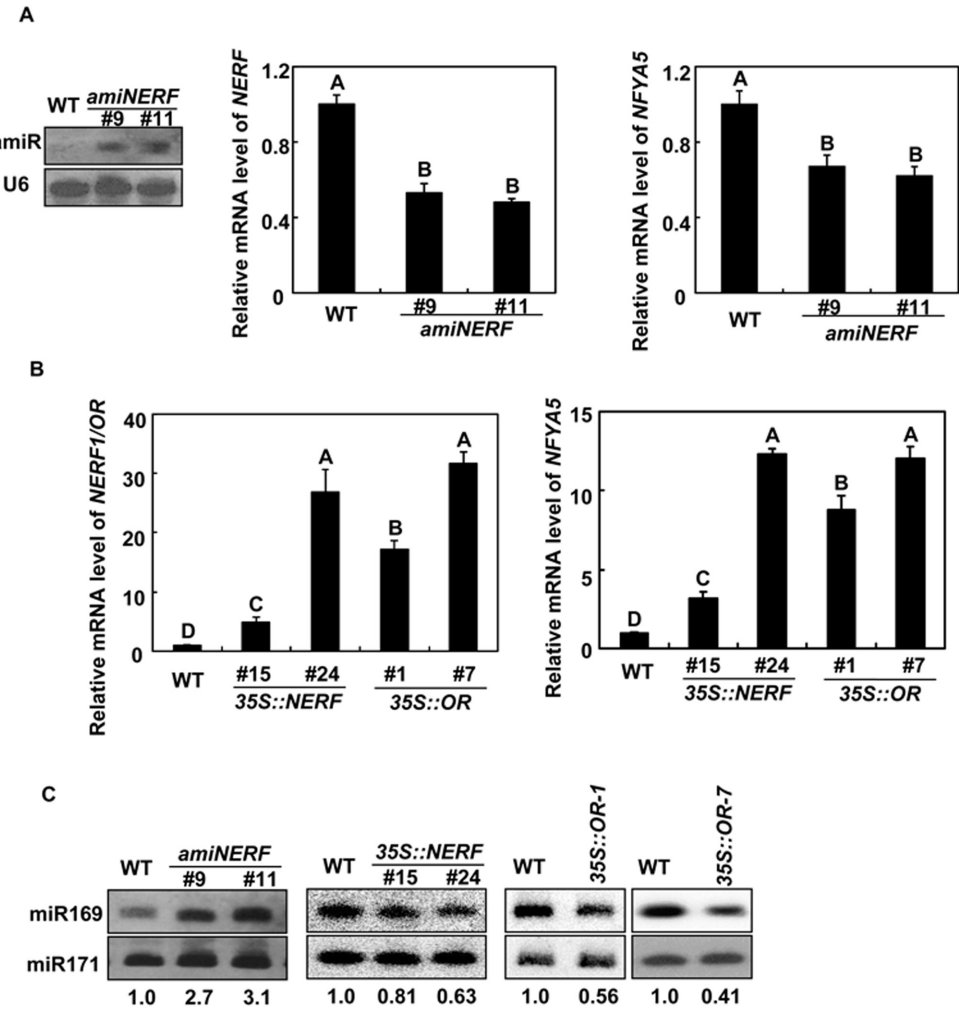

Figure 3. *NFYA5* mRNA abundance was positively affected by *NERF* transcripts. (**A**) *NFYA5* mRNA levels decreased in *amiNERF* transgenic plants. Small RNA gel blot analysis of artificial-miRNA in *amiNERF* transgenic plants. U6 was used as a loading control. The corresponding *NERF* and *NFYA5* expression levels were analyzed by real-time RT-PCR. Quantifications were normalized to that of *Tub4*. Error bars represent standard errors ($n = 3$). LSD test was used to test differences between treatments. Means with the same letter were not significantly different at $P < 0.01$. (**B**) *NFYA5* mRNA levels increased in *35S::NERF* and *35S::OR* transgenic plants. The *NERF*, *OR*, and *NFYA5* expression levels were analyzed by real-time RT-PCR. Quantifications were normalized to that of *Tub4*. Error bars represent standard errors ($n = 3$). LSD test was used to test differences between treatments. Means with the same letter were not significantly different at $P < 0.01$. (**C**) Expression analysis of miRNA169 accumulation in *35S::NERF*, *35S::OR* and *amiNERF* transgenic plants. A 20-μg quantity of small RNA from each sample was loaded per lane and hybridized with ^{32}P-labeled probe corresponding to the sequence of miR169. miR171 was used as a loading control. Numbers below each lane indicate the expression level of miR169 relative to miR171.

nucleotides 10 and 11 of miR169 was identified, demonstrating that miR169 can direct *NFYA5* mRNA cleavage. To our surprise, four additional cleavage sites in the *NFYA5* mRNA were identified, and one of these was the most frequent cleavage site (10 of 20). No other conserved miRNAs except for miR169 from the *Arabidopsis* small RNA database were predicted to target *NFYA5* (http://mpss.udel.edu/at_sRNA/), indicating that siRNANERF does exist in *OR* and can direct the cleavage of *NFYA5* mRNA.

To determine which pathway components might be involved in the biogenesis of siRNANERF, we checked the expression of siRNANERF in mutants defective in various proteins known to be required for biogenesis of specific types of small RNAs; the attempt failed (Supplementary Figure S4), perhaps because of cross-hybridization between the siRNANERF and miRNA169 (Supplementary Figure S3) or because of the low abundance of the siRNANERF. The generation of small RNAs depends on different DICER-like (DCL) proteins in plants. DCL2 is believed to generate viral siRNAs (30); DCL3 forms heterochromatic siRNAs (30); and DCL4 is required for ta-siRNA biogenesis (31,32). To investigate the possible roles of DCLs in the generation of siRNANERF, we overexpressed *OR* in *dcl2/3/4* triple mutants (Supplementary Figure S5). The mRNA level of *NFYA5* did not substantially change despite overexpression of *OR* in the *dcl2/3/4* triple mutant (Figure 5C). As expected, the accumulation of siRNANERF observed in *35S::NERF* transgenic plants was blocked in *dcl2/3/4 35S::OR* plants, and the expression of miR169 did not significantly differ among *dcl2/3/4* and transgenic plants (Figure 5A and D). These results suggested that

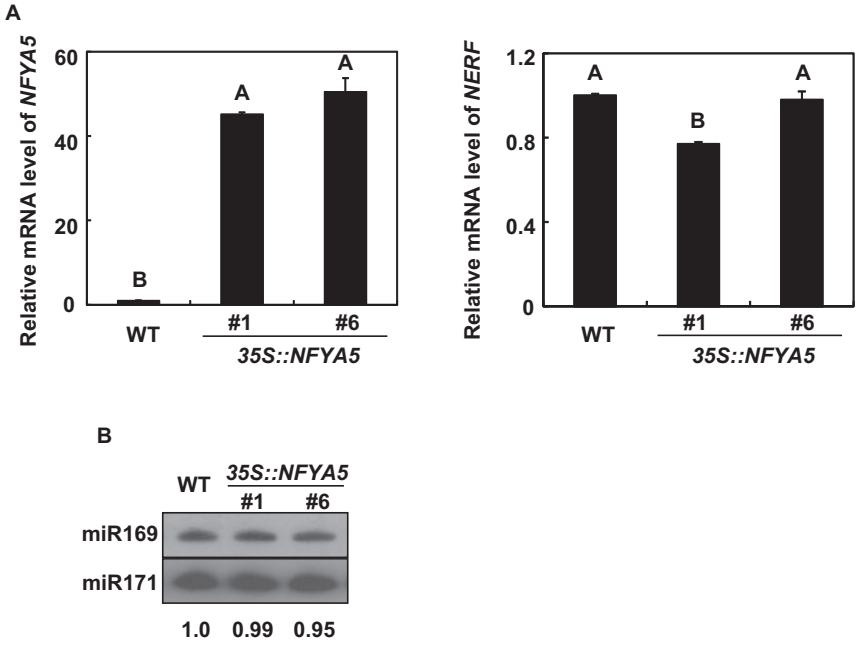

Figure 4. *NFYA5* overexpression did not affect *NERF* abundance. (**A**) Detection of *NFYA5* and *NERF* transcripts in *35S::NFYA5* transgenic plants by real-time RT-PCR. Quantifications were normalized to the expression of *Tub4*. Error bars represent standard errors ($n = 3$). LSD test was used to test differences between treatments. Means with the same letter were not significantly different at $P < 0.01$. (**B**) Accumulation of miR169 in *35S::NFYA5* transgenic plants. A 20-μg quantity of small RNA from each sample was loaded per lane and hybridized with ^{32}P-labeled probe corresponding to the sequence of miR169. miR171 was used as a loading control. Numbers below each lane indicate the expression level of miR169 relative to miR171.

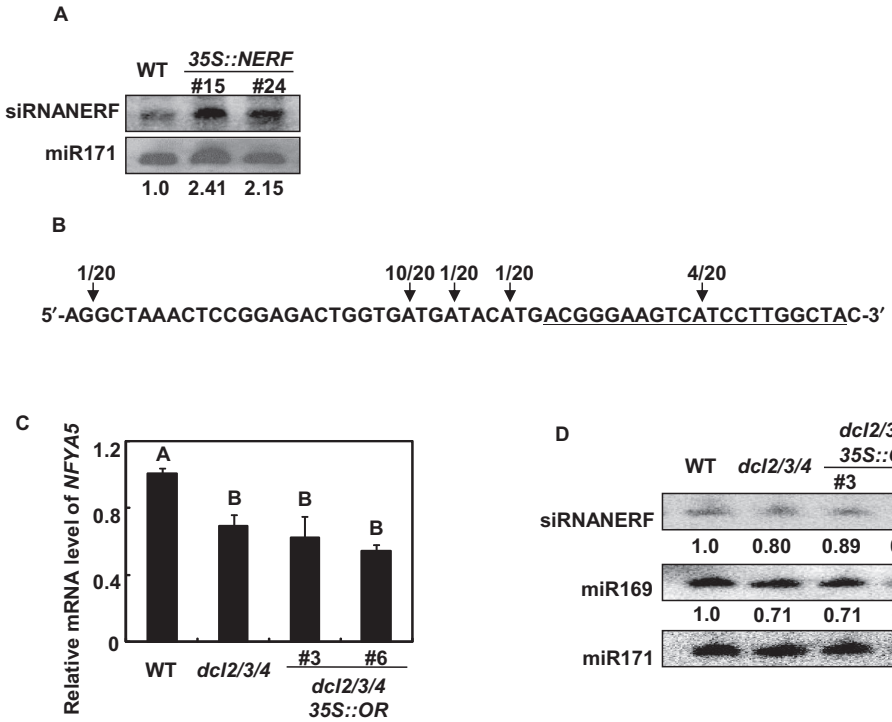

Figure 5. siRNANERF biogenesis. (**A**) siRNANERF accumulated in *35S::NERF* transgenic plants. A 20-μg quantity of small RNA from each sample was loaded per lane and hybridized with ^{32}P-labeled *OR* cDNA probe. miR171 was used as a loading control. Numbers below each lane indicate the expression level of siRNANERF relative to miR171. (**B**) *NFYA5* mRNA cleavage sites detected by 5′ RACE. Numbers indicate the frequency of cleavage at each site. Target site of miRNA 169 was underlined. (**C**) Detection of *NFYA5* gene transcripts in *dcl2/3/4 35S::OR* transgenic plants by real-time RT-PCR. Quantifications were normalized to the expression of *Tub4*. Error bars represent standard errors ($n = 3$). LSD test was used to test differences between treatments. Means with the same letter were not significantly different at $P < 0.01$. (**D**) Detection of siRNANERF and miR169 in *dcl2/3/4 35S::OR* transgenic plants. A 20-μg quantity of small RNA from each sample was loaded per lane and hybridized with ^{32}P-labeled probe corresponding to the sequence of *OR* cDNA or miR169. miR171 was used as a loading control.

DCL2, DCL3, or/and DCL4 should affect the biogenesis of siRNANERF.

siRNANERF produced from *OR*

To avoid the interference of artificial miRNAs generated in *amiNERF* transgenic lines, we generated a small RNA library from *35S::OR* transgenic plants and sequenced the library by Solexa high-throughput sequencing technology. The small RNA library yielded more than 11 million raw reads. Approximately 95% of the raw reads remained after 3′ and 5′ adaptor trimming, and more than 8 million reads could be perfectly mapped to the *Arabidopsis* genome (the Arabidopsis Information Resource 9). Sequences that could not be mapped to the *Arabidopsis* genome were discarded, and only those that perfectly mapped were analyzed further. Of these, 960 sequences representing 323 unique siRNANERF could be perfectly mapped to *OR* (Supplementary Table S2). Among the total sequence reads matching *OR*, 21-nt small RNAs were dominant (Supplementary Figure S6), which was in consistent with the small RNA molecular weight detected by *OR* cDNA.

siRNANERF could originate from both positive and negative strands, and about 58% of them were from the negative strand. They were scattered along the *OR*, and two active loci producing siRNANERF (200–230 bp and 250–280 bp) were identified (Supplementary Figure S1). Interestingly, one of the two loci (200–230 bp) partially overlapped with the miR169 binding sites in *NFYA5* (Supplementary Figure S1). The sequences of some siRNANERF that originated from the positive strand of *OR* are similar to those of miR169, especially at the 5′ end of mature miR169 (Figure 6A). We also found that some siRNANERF were partially complementary to miR169 (Supplementary Figure S7). To further characterize the function of these siRNAs, we cloned the 195- to 280-bp cDNA in *OR* containing the two loci and overexpressed it in *Arabidopsis* (Supplementary Figure S1). Two transgenic lines designated as *35S::ORC* (*OR* Core) were chosen for further analysis (Figure 6B). siRNANERF abundance and *NFYA5* transcripts also increased in *35S::ORC* transgenic plants, and correspondingly, the miR169 expression levels decreased (Figure 6B), which was similar to the phenomenon observed in *35S:NERF* and *35S::OR* transgenic plants. These results suggested that the functions of *ORC* containing siRNAs analogous/complementary to miR169 and *OR* are at least partially similar to that of *OR*.

Overexpression of *NERF*, like overexpression of *NFYA5*, increases drought resistance of *Arabidopsis*

The expression of *NERF* in guard cells (Figure 2B) and accumulation of *NFYA5* transcripts in *35S::NERF* and *35S::OR* transgenic plants prompted us to analyze the role of *NERF* in drought resistance in *Arabidopsis*. Five transgenic lines (#15, #17, #20, #21 and #24) were chosen for further analysis based on their expression level (Figure 7A). WT and *35S::NERF* plants were grown for 3 weeks in soil and were then subjected to water withholding for 14 days. Most WT plants wilted and their leaves became purple, while the *35S::NERF* plants remained turgid and their leaves remained green (Figure 7B). The results suggested that *35S::NERF* plants might wilt more slowly than WT plants because the former plants depleted soil water more slowly. To investigate this possibility, stomatal apertures were measured in leaves of *35S::NERF-20* and WT plants grown in soil. When water was not withheld, the stomatal aperture index of *35S::NERF-20* leaves was 0.34, which was nearly 30% smaller than that of the WT (Figure 7C). When water was withheld for 14 days, the stomatal aperture index of *35S::NERF-20* leaves declined to 0.24, which was ∼32% smaller than that of the WT. These data indicated that the ability of the transgenic plants to remain turgid when water was withheld could be attributed at least in part to an increased ability to close stomata and reduce transpiration.

amiNERF plants are hypersensitive to drought stress

In contrast to *35S::NERF* transgenic plants, *amiNERF* plants were hypersensitive to drought stress (Figure 8). After water had been withheld for 9 days, most of the *amiNERF* plants appeared more dehydrated than the WT (Figure 8A). The stomatal aperture index of WT leaves declined from 0.48 to 0.39, which was ∼20% smaller than that of the *amiNERF* plants (Figure 8B). The results suggest that adequate expression of *NERF* is required for drought resistance and that *NERF* and *NFYA5* have similar functions with respect to stomatal closure and drought stress.

DISCUSSION

Gene regulation under abiotic stress is mediated by multiple cascades of transcription factors (33). In each of these cascades, a transcription factor gene is induced or activated, which in turn activates or represses downstream target genes important for abiotic resistance. NFYA5 regulates the expression of stress-responsive genes (e.g. the genes that encode subunit of cytochrome b6-f complex, GST, peroxidases and oxidoreductase family proteins), and contributes to one of these abiotic stress-responsive transcriptional cascades (19). The transcriptional levels of *NFYA5* were positively related to *NERF* mRNA abundance, and *35S::NERF* transgenic- and *amiNERF* knock-down plants showed similar drought response phenotypes as *NFYA5* overexpression lines or *nfya5* loss-of-function mutants in drought responses. These results suggest that *NERF* and *NFYA5* are involved in the same gene regulon and that *NERF* acts upstream in this regulon.

The similar expression pattern (leaf and root vascular systems, guard cells, and flowers) and nuclear localization of *NERF* and *NFYA5* satisfy the basic prerequisites for the formation of double-stranded DNA to produce siRNAs. Deep sequencing of a small RNA library constructed from *35S::OR* transgenic plants verified the existence of the siRNAs that originated from *OR*. Because of cross-hybridization with miRNA169, we were unable to identify the biogenesis pathway of siRNA that originated from *OR*. We first deduced that these siRNAs belonged to nat-siRNA. Unlike NaCl-inducible nat-siRNASRO5 and pathogen-inducible nat-siRNAATGB2, which have specific sequences that regulate corresponding target genes (12,13), the siRNAs in our small RNA library had different se-

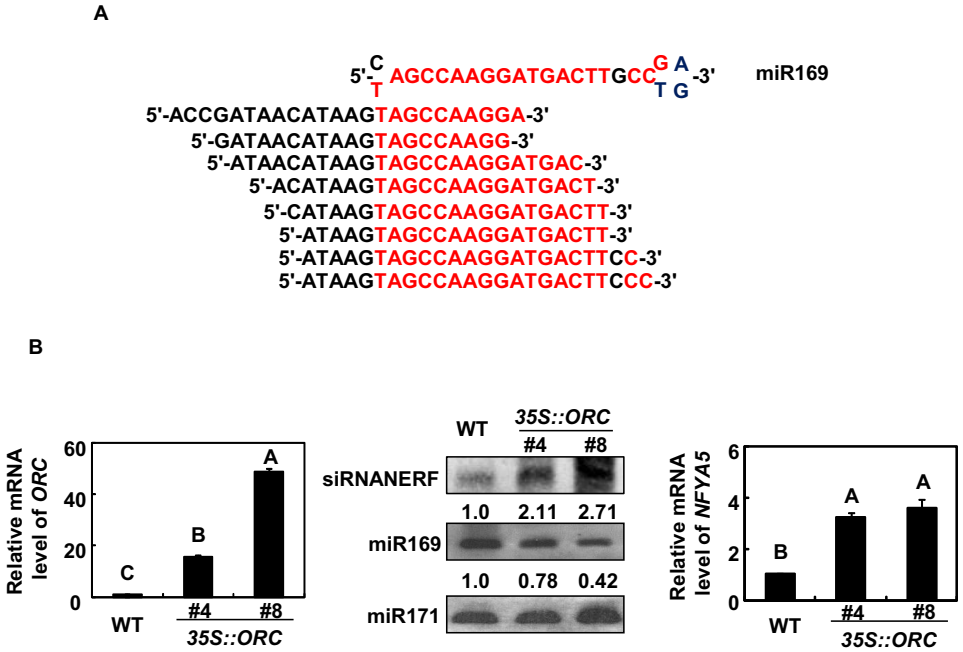

Figure 6. siRNANERF originated from *OR*. (**A**) Diagram of siRNANERF that originated from *OR* and had a sequence similar to that of miR169. (**B**) *NFYA5* mRNA levels also increased in *35S::ORC* transgenic plants. Detection of *ORC* and *NFYA5* transcripts in *35S::ORC* transgenic plants by real-time RT-PCR. Quantifications were normalized to the expression of *Tub4*. Error bars represent standard errors ($n = 3$). For analysis of siRNANERF and miR169 accumulation in *35S::ORC* transgenic plants, 20 μg quantity of small RNA from each sample was loaded per lane and hybridized with ^{32}P-labeled probe corresponding to the sequence of miR169 or *OR* cDNA. miR171 was used as a loading control. Numbers below each lane indicate the expression level of miR169/siRNANERF relative to miR171. LSD test was used to test differences between treatments. Means with the same letter were not significantly different at $P < 0.01$.

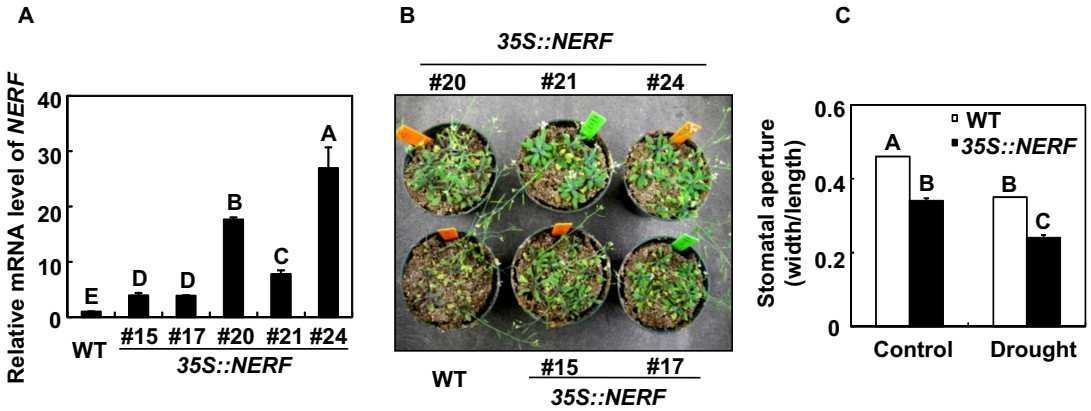

Figure 7. Increased drought resistance in *35S::NERF* transgenic plants. (**A**) Detection of *NERF* mRNA in *35S::NERF* transgenic plants by real-time RT-PCR. Quantifications were normalized to the expression of *Tub4*. Error bars represent standard errors ($n = 3$). LSD test was used to test differences between treatments. Means with the same letter were not significantly different at $P < 0.01$. (**B**) Drought resistance of *35S::NERF* plants (#15, #17, #20, #21 and #24). WT and *35S::NERF* plants were grown in soil with sufficient water for 3 weeks, and then the water was withheld for 14 days. Photographs of representative plants are shown. (**C**) Measurements of the stomatal apertures in WT and *35S::NERF* transgenic plants. Values are mean ratios of width to length ± SE of three independent experiments ($n = 60$–80). LSD test was used to test differences between treatments. Means with the same letter were not significantly different at $P < 0.01$.

quences. They were scattered along the *OR* and did not arrange in phase as did the small RNAs of nat-siRNASRO5 (12). Zhang *et al.* reported that the generation of 20- to 22-nt nat-siRNAs depended on DCL1 and that generation of the 23- to 28-nt nat-siRNAs depended on DCL3 (11). The biogenesis of sperm-specific nat-siRNAKPL was also demonstrated to be processed by the DCL1–HYL1 complex (14). In our research, the accumulation of siRNANERF and the induction of *NFYA5* in *35S::NERF* transgenic plants were blocked in *dcl2/3/4*, which strongly indicated that DCL1 was not the major effector regulating siRNANERF production and that DCL2, DCL3, DCL4 or some combination, is involved in the biogenesis of siRNANERF.

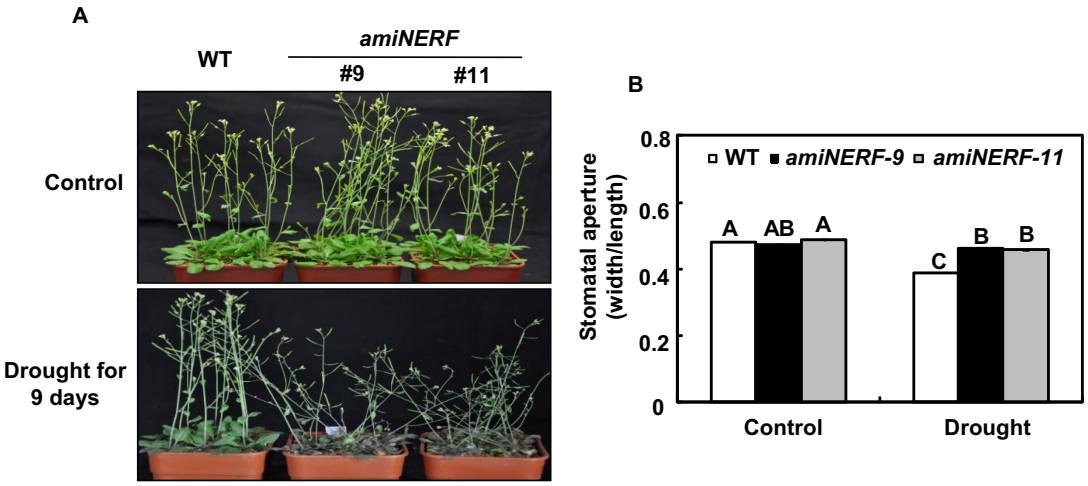

Figure 8. *amiNERF* plants were more sensitive to drought stress. (**A**) Response of *amiNERF* transgenic plants to drought stress. WT and *amiNERF* transgenic plants were grown in soil with sufficient water for 3 weeks, and then the water was withheld for 9 days. Photographs are of representative plants. Control, without water withholding. (**B**) Stomatal aperture size in WT and *amiNERF* transgenic plants. Values are mean ratios of width to length ± SE of three independent experiments ($n = 60$–80). LSD test was used to test differences between treatments. Means with the same letter were not significantly different at $P < 0.01$.

Interestingly, the sequences of some siRNANERF were similar to that of miR169, especially at the 5′ end of mature miR169. Pairing to the miRNA 5′ region was crucial for miRNA-guided cleavage of target genes (34,35). In humans, *BACE1* antisense transcript and miR-485–5p ncRNAs competed for binding to the exonic region of *BACE1* mRNA, and covering of the miRNA binding site by *BACE1* antisense transcript eliminated the miRNA-induced translational repression and *BACE1* mRNA decay (8). The siRNANERF with similar sequence to that miR169 might also compete for *NFYA5*-targeting miR169 in *Arabidopsis*. The inference is based on: (1) four additional cleavage sites in addition to that of miR169 in the *NFYA5* mRNA were identified; and (2) miR169 expression was not affected when siRNANERF were blocked in dcl2/3/4 triple mutants. Unexpectedly, we also detected that some siRNANERF were partially complementary to miR169. When the sequence complementarity between a siRNA and its target is extensive, the inhibition that results is said to involve 'target mimicry'. For example, a 23-nt motif in *IPS1*, *At4* and other members in this family has extensive sequence complementarity with miR399, and this leads to substantial inhibition of miR399 activity (36). In contrast, the siRNANERF that originated from the negative strand of *NERF* has only partial complementarity with miR169. This partial complementarity did not affect the expression of miRNA169 according to the results obtained with *35S::NFYA5* transgenic plants with UTR. Determining the physiological functions and regulation of these siRNAs therefore requires further research.

NFYA5 transcripts accumulated and miR169 expression down-regulated in *35S::NERF*, *35S::OR* and *35S::ORC* transgenic plants, while the opposite were true for *amiNERF* knock-down mutants, which strongly indicated that siRNANERF interacts with miR169. We propose the following model for the co-functioning of siRNANERF and miR169. Like *BACE1-AS* in human, siRNANERF originating from *OR* between *NERF* and *NFYA5* could mask of and/or compete with the *NFYA5*-targeting miR169 and thereby impair the miR169-guided cleavage of *NFYA5*, leading to *NFYA5* accumulation under drought stress and, thereby to enhance drought tolerance in *Arabidopsis*. This regulatory model might be applied to other natural antisense transcripts with positively correlated expression patterns.

SUPPLEMENTARY DATA

Supplementary Data are available at NAR Online.

FUNDING

National Science Foundation of China [31370303]; National High-Tech R & D Program [2012AA10A306]; Core Research Budget of the Non-profit Governmental Research Institution [2014001 to W.X.L.]. Funding for open access charge: National Science Foundation of China [31370303].
Conflict of interest statement. None declared.

REFERENCES

1. Vaucheret,H. (2006) Post-transcriptional small RNA pathways in plants: mechanisms and regulations. *Genes Dev.*, **20**, 759–771.
2. Rajagopalan,R., Vaucheret,H., Trejo,J. and Bartel,D.P. (2006) A diverse and evolutionarily fluid set of microRNAs in *Arabidopsis thaliana*. *Genes Dev.*, **20**, 3407–3425.
3. Zhou,X., Sunkar,R., Jin,H., Zhu,J.K. and Zhang,W. (2009) Genome-wide identification and analysis of small RNAs originated from natural antisense transcripts in *Oryza sativa*. *Genome Res.*, **19**, 70–78.
4. Faghihi,M.A. and Wahlestedt,C. (2009) Regulatory roles of natural antisense transcripts. *Nat. Rev. Mol. Cell Biol.*, **10**, 637–643.
5. Henz,S.R., Cumbie,J.S., Kasschau,K.D., Lohmann,J.U., Carrington,J.C., Weigel,D. and Schmid,M. (2007) Distinct expression patterns of natural antisense transcripts in Arabidopsis. *Plant Physiol.*, **144**, 1247–1255.
6. Osato,N., Yamada,H., Satoh,K., Ooka,H., Yamamoto,M., Suzuki,K., Kawai,J., Carninci,P., Ohtomo,Y., Murakami,K. *et al.*

(2003) Antisense transcripts with rice full-length cDNAs. *Genome Biol.*, **5**, R5.
7. Wang,X.J., Gaasterland,T. and Chua,N.H. (2005) Genome-wide prediction and identification of *cis*-natural antisense transcripts in *Arabidopsis thaliana*. *Genome Biol.*, **6**, R30.
8. Faghihi,M.A., Zhang,M., Huang,J., Modarresi,F., VanderBrug,M.P., Nalls,M.A., Cookson,M.R., St-Laurent,G. and Wahlestedt,C. (2010) Evidence for natural antisense transcript-mediated inhibition of microRNA function. *Genome Boil.*, **11**, R56.
9. Jin,H., Vacic,V., Girke,T., Lonardi,S. and Zhu,J.K. (2008) Small RNAs and the regulation of cis-natural antisense transcripts in Arabidopsis. *BMC Mol. Biol.*, **9**, 6.
10. Ghildiya,M. and Zamore,P.D. (2009) Small silencing RNAs: an expanding universe. *Nat. Rev. Genet.*, **10**, 94–108.
11. Zhang,X., Xia,J., Li,Y.E., Barrera-Figuero,B.E., Zhou,X., Gao,S., Lu,L., Niu,D., Chen,Z., Leuge,C. *et al.* (2012) Genome-wide analysis of plant nat-siRNAs reveals insights into their distribution, biogenisis and function. *Genome Biol.*, **13**, R20.
12. Borsani,O., Zhu,J., Verslues,P.E., Sunkar,R. and Zhu,J.K. (2005) Endogenous siRNAs derived from a pair of natural *cis*-antisense transcripts regulate salt tolerance in *Arabidopsis*. *Cell*, **123**, 1279–1291.
13. Katiyar-Agarwa,S., Morgan,R., Dahlbeck,D., Borsani,O., Villegas,A.J., Zhu,J.K., Staskawicz,B.J. and Jin,H.L. (2006) A pathogen-inducible endogenous siRNA in plant immunity. *Proc. Natl. Acad. Sci. U.S.A.*, **103**, 18002–18007.
14. Ron,M., Saez,M.A., Williams,L.E., Fletcher,J.C. and McCormick,S. (2010) Proper regulation of a sperm-specific *cis*-nat-siRNA is essential for double fertilization in *Arabidopsis*. *Genes Dev.*, **24**, 1010–1021.
15. Jen,C.H., Michalopoulos,I., Westhead,D.R. and Meyer,P. (2005) Natural antisense transcripts with coding capacity in *Arabidopsis* may have a regulatory role that is not linked to double-stranded RNA degradation. *Genome Biol.*, **6**, R51.
16. Zhan,S. and Lukens,L. (2013) Protein-coding cis-natural antisense transcripts have high and broad expression in Arabidopsis. *Plant Physiol.*, **161**, 2171–2180.
17. Zhu,J.K. (2002) Salt and drought stress signal transduction in plants. *Annu. Rev. Plant Biol.* **53**, 247–273.
18. Bohnert,H.J., Gong,Q., Li,P. and Ma,S. (2006) Unraveling abiotic stress tolerance mechanisms–getting genomics going. *Curr. Opin. Plant Biol.*, **9**, 180–188.
19. Li,W.X., Oono,Y., Zhu,J., He,X.J., Wu,J.M., Iida,K., Lu,X., Cui,X., Jin,H. and Zhu,J.K. (2008) The *Arabidopsis* NFYA5 transcription factor is regulated transcriptionally and posttranscriptionally to promote drought resistance. *Plant Cell*, **20**, 2238–2251.
20. Zhang,Y., Yang,C., Li,Y., Zheng,N., Chen,H., Zhao,Q., Gao,T., Guo,H. and Xie,Q. (2007) SDIR1 is a RING Finger E3 ligase that positively regulates stress-responsive abscisic acid signaling in *Arabidopsis*. *Plant Cell*, **19**, 1912–1929.
21. Lee,H.K., Cho,S.K., Son,O., Xu,Z., Hwang,I. and Kim,W.K. (2009) Drought stress-induced Rma1H1, a RING membrane-anchor E3 ubiquitin ligase homolog, regulates aquaporin levels via ubiquitination in transgenic *Arabidopsis* plants. *Plant Cell*, **21**, 622–6410.
22. Schwab,R., Ossowski,S., Riester,M., Warthmann,N. and Weigel,D. (2006) Highly specific gene silencing by artificial microRNAs in *Arabidopsis*. *Plant Cell*, **18**, 1121–1133.
23. Clough,S.J. and Bent,A.F. (1998) Floral dip: a simplified method for *Agrobacterium*-mediated transformation of *Arabidopsis thaliana*. *Plant J.*, **16**, 735–743.
24. Ramakers,C., Ruijter,J.M., Deprez,R.H. and Moorman,A.F. (2003) Assumption-free analysis of quantitative real-time polymerase chain reaction (PCR) data. *Neurosci. Lett.*, **339**, 62–66.
25. Sunkar,R. and Zhu,J.K. (2004) Novel and stress-regulated microRNAs and other small RNAs from Arabidopsis. *Plant Cell*, **16**, 2001–2019.
26. Xie,Q., Guo,H.S., Dallman,G., Fang,S., Weissman,A.M. and Chua,N.H. (2002) SINAT5 promotes ubiquitin-related degradation of NAC1 to attenuate auxin signals. *Nature*, **419**, 167–170.
27. Combier,J.P., Frugier,F., Billy,F., Boualem,A., El-Yahyaoui,F., Moreau,S., Vernie,T., Ott,T., Gamas,P., Crespi,M. *et al.* (2006) *MtHAP2–1* is a key transcriptional regulator of symbiotic nodule development regulated by microRNA169 in *Medicago truncatula*. *Genes Dev.*, **20**, 3084–3088.
28. Meyers,B.C., Axtell,M.J., Bartel,B., Bartel,D.P., Baulcombe,D., Bowman,J.L., Cao,X., Carrington,J.C., Chen,X., Green,P.J. *et al.* (2008) Criteria for annotation of plant microRNAs. *Plant Cell*, **20**, 3186–3190.
29. Zuker,M. (2003) Mfold web server for nucleic acid folding and hybridization prediction. *Nucleic Acids Res.*, **31**, 3406–3415.
30. Xie,Z., Johansen,L.K., Gustafson,A.M., Kasschau,K.D., Lellis,A.D., Zilberman,D., Jacobsen,S.E. and Carrington,J.C. (2004) Genetic and functional diversification of small RNA pathways in plants. *PLoS Biol.*, **2**, e104.
31. Dunoyer,P., Himber,C. and Voinnet,O. (2005) DICER-LIKE 4 is required for RNA interference and produces the 21-nucleotide small interfering RNA component of the plant cell-to-cell silencing signal. *Nat. Genet.*, **37**, 1356–1360.
32. Xie,Z., Allen,E., Fahlgren,N., Calamar,A., Givan,S.A. and Carrington,J.C. (2005) Expression of Arabidopsis *MIRNA* genes. *Plant Physiol.*, **138**, 2145–2154.
33. Zhu,J.K. (2002) Salt and drought stress signal transduction in plants. *Annu. Rev. Plant Biol.*, **53**, 247–273.
34. Mallory,A.C., Reinhart,B.J., Jones-Rhoades,M.W., Tang,G., Zamore,P.D., Baryon,M.K. and Bartel,D.P. (2004) MicroRNA control of *PHABULOSA* in leaf development: importance of pairing to the microRNA 5′ region. *EMBO J.*, **23**, 3356–3364.
35. Bartel,D.P. (2009) MicroRNAs target recognition and regulatory functions. *Cell*, **136**, 215–233.
36. Franco-Zorrilla,J.M., Valli,A., Todesco,M., Mateos,I., Puga,M.I., Rubio-Somoza,I., Leyva,A., Weigel,D., García,J.A. and Paz-Ares,J. (2007) Target mimicry provides a new mechanism for regulation of microRNA activity. *Nat. Genet.*, **39**, 1033–1037.